

Electron and hole capture in multiple-quantum-well structures

D. Morris,* B. Deveaud, A. Regreny, and P. Auvray
France Telecom, CNET, Lannion B, 22301 Lannion, France
 (Received 21 December 1992)

We have studied a series of modified GaAs/ $\text{Al}_x\text{Ga}_{1-x}\text{As}$ multiple-quantum-well structures, where increased capture times are obtained owing to the engineering of the band configuration. Both electron and hole capture times have been measured as a function of well width. Hole capture times are fast (typically 10 ps) and depend weakly on the structure. Electron capture times are shown to vary between 2 and 120 ps for well widths covering the whole range between 30 and 100 Å. This variation and the short time observed at resonance, when the barrier and the well levels are separated by 1 LO-phonon energy, demonstrate the importance of quantum-mechanical electron capture processes.

Carrier capture mechanisms play a crucial role in the performance of quantum-well- (QW) based devices such as lasers and intersubband photodetectors. For QW lasers, a higher gain and thus a lower threshold current are obtained owing to efficient carrier capture into the active layer.¹ For photodetectors, a long carrier capture time favors the photocarrier collection and thus improves the responsivity of the devices.² For practical reasons it is thus important to understand the carrier capture mechanisms.

In idealized (free of defects) quantum-well structures, emission of LO phonons is the main carrier capture mechanism. The LO-phonon scattering rate depends on two main terms: the Fröhlich matrix element, which gives a $1/q^2$ dependence (where q is the wave vector of the emitted phonon) and the overlap of the initial and final wave functions squared. Published quantum-mechanical calculations³⁻⁶ predict strong resonances (variation of two orders of magnitude) of the carrier capture time as a function of well width. A first kind of resonance is expected when the energy difference between the barrier ground state and one of the QW levels equals the LO-phonon energy, because the phonon wave vector q is small. The second kind of resonance originates from the increased wave-function overlap when a continuum state is approaching the barrier band-edge energy. Oscillations of the QW photoluminescence (PL) intensity with well width, due to variations of the carrier trapping efficiency, has been reported in cw luminescence.⁷ However, this experiment does not give a direct measure of the carrier capture times. Such a measure can be obtained by time-resolved PL techniques but, among the various experiments reported in the literature,⁸⁻¹⁰ none gives any evidence for resonant capture mechanisms. On the other hand, some recent papers^{11,12} suggest that for conditions prevailing in QW lasers, a quantum-mechanical description is not the appropriate picture for carrier transfer into the quantum well. More experiments are therefore needed for a better understanding of the capture mechanisms.

We have first investigated the quantum-mechanical capture mechanisms by studying a complete series of multiple-quantum-well (MQW) structures with 200-Å-thick barriers and well widths covering the whole range

between 40 and 120 Å.¹³ Both electrons and holes are found to be captured in less than 3 ps. The absence of long times is explained theoretically by the combination of different capture mechanisms (LO-phonon scattering and impurity scattering) and by the effect of carrier spreading in energy over a Maxwell-Boltzmann distribution. The same theory also predicts very short times (≈ 100 fs) when the electrons are scattered by $q=0$ phonons ($L_z \approx 60$ and 110 Å, for $x_{\text{Al}}=0.25$ in the barriers). These short times cannot be observed in luminescence because the electrons, created at 2.05 eV, first scatter to the X valley and only return slowly to the Γ valley (≈ 2 ps). An experimental approach, described below, may be chosen to overcome this limitation.

In the present paper, we have studied a different series of MQW samples by the time-resolved PL technique. Compared to the usual MQW's, the band configuration of the structures has been modified in order to increase the electron capture times above the limiting value of 2 ps. We have considered different possible structures (compatible with our epitaxy facilities) that reduce the barrier and well wave-function overlap and thus give longer capture times. This can be obtained by increasing the barrier

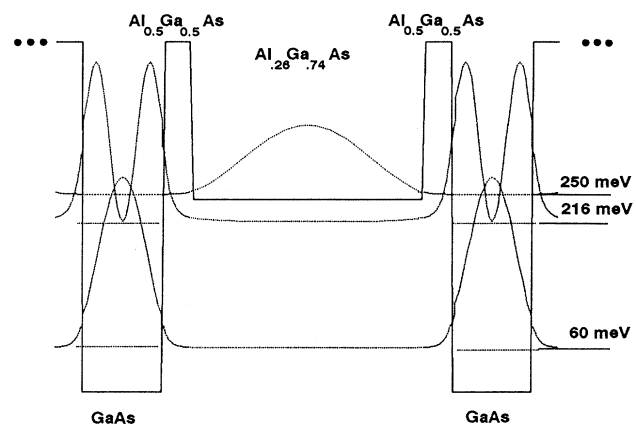


FIG. 1. Schematic electron band configuration of our samples. The energy and the wave functions squared of the first three levels are plotted for the 73-Å sample (nearest-resonant condition).

thickness up to the carrier mean-free-path (MFP) limit. In high-quality $\text{Al}_x\text{Ga}_{1-x}\text{As}$, the electron MFP is ≤ 500 Å, and this upper barrier thickness limit only increases the minimum electron capture times to about 300 fs. The coherence length for holes estimated from transport measurement is at least a factor of 3 lower than the electron MFP. We have chosen to keep the 200-Å barrier thickness but to modify the barrier configuration by adjoining edge spikes on either side of the wells (see Fig. 1). The use of such a band configuration for capture studies was first proposed by Fujiwara *et al.*¹⁴ The wave-function overlap is reduced by adjusting the height (the Al content) and the width of these edge spikes. The only restriction is the position of the X levels which have to be sufficiently above the barrier ground state; otherwise direct electron capture by these X valleys complicates the picture. In this work, a 23-Å-thick and a $x_{\text{Al}}=0.50$ $\text{Al}_x\text{Ga}_{1-x}\text{As}$ spike layers have been chosen to obtain an increase of the electron capture times by roughly a factor of 15. Strong oscillations of electron capture times as a function of well width and a 1.5-ps value at resonance are predicted for such structures.

Our samples, grown by molecular-beam epitaxy, consist of 20 repetitions of the structure shown in Fig. 1. Also shown in Fig. 1 are the electron wave functions squared corresponding to the first three electron levels for the 70-Å sample. The thin spike layers consist of an $\text{Al}_{0.5}\text{Ga}_{0.5}\text{As}$ alloy obtained by the deposition of four periods of GaAs/AlAs monolayer superlattice. The structural parameters (alloy composition and thicknesses of the different layers) are deduced from a fit to the x-ray diffraction patterns and to the observed energies of the PL transitions. Table I gives a list of the samples together with their structural parameters. For all samples, the barrier thicknesses are about 200 Å and the spike thickness about 23 Å. Photoluminescence spectra are obtained at low temperature (100 K) by an up-conversion

TABLE I. List of the samples together with the experimental and theoretical data points.

Sample no.	$x_{\text{Al}} \pm 0.005$	Well width (Å)	δE_{el} (meV) ± 5	Experimental data		Theory
				τ^{hole} (ps)	τ^{el} (ps)	τ^{el} (ps)
1	0.305	29	103	$8 \pm 1^{\text{a}}$	$50 \pm 10^{\text{a}}$	35
2	0.310	53	202^{b}	10 ± 2	10 ± 2	24
3	0.290	77	77	8 ± 1	62 ± 15	28
4	0.255	50	143	9 ± 2	118 ± 30	145
5	0.275	58	180^{b}	12 ± 2	21 ± 7	38
6	0.270	70	31	10 ± 2	3 ± 2	5
7	0.260	73	34	9 ± 2	2 ± 1	3
8	0.270	84	81	13 ± 2	55 ± 8	39
9	0.275	96	117	15 ± 2	41 ± 8	57

^aThe experimental errors have been estimated from the fitting procedure.

^bA barrier wave-function buildup in the well is expected for those samples.

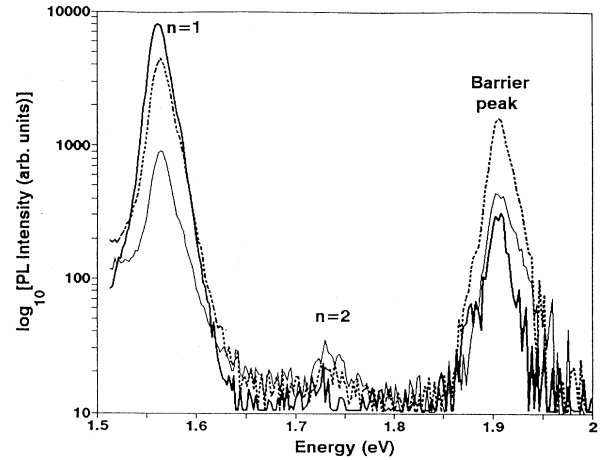


FIG. 2. Typical luminescence spectra measured at 100 K, at three time delays for the 84-Å sample. Solid line, 1 ps; dashed line, 3 ps; and heavy solid line, 20 ps.

technique with a 600-fs resolution. The sensitivity of the experiment allows the observation of the barrier and well luminescence without any band-filling effects; the excitation density corresponds to $2 \times 10^{10} \text{ cm}^{-2}$ per well.

Typical luminescence spectra are shown in Fig. 2 at three different delays (1, 3, and 20 ps) for the 84-Å sample. These spectra have been obtained at relatively high excitation density in order to evidence the $n=2$ transition. The $n=1$ and 2 quantum-well-luminescence (QWL) peaks are observed at 1.570 and 1.735 eV, respectively. On the high-energy side of the spectrum, the barrier-luminescence (BL) peak is observed at 1.905 eV. The BL corresponds to electron-hole recombination of carriers at the barrier ground states, and the QWL comes from recombination of carriers at the QW ground states. Even for a time delay as short as 1 ps, a Maxwell-Boltzmann distribution of carriers is observed;¹⁵ the effective carrier temperature is 170 K at 1 ps and reaches 100 K in about 3 ps. This fast cooling process increases the QWL and the BL at short times. Carrier capture by the quantum well (occurring in few tens of ps) gives rise to an increase of the QWL as well as a decrease of the BL peak.

The intensities of the transitions are proportional to the hole and electron populations of the related levels. The dynamical behavior of the PL signals gives information on the different characteristic times. The BL decays roughly with the fastest capture times. The QWL rises upon cooling of the carriers photoexcited in the wells, and upon capture of carriers coming from the barriers. Figures 3(a) and 3(b) show the temporal behavior of the well and barrier PL signals. These figures compare the spectra of three samples with well widths close to the value where a resonance in the electron capture rate is expected. The intensity of the BL peak decays exponentially with time over two decades. On the other hand, the QWL rise time shows a complex behavior. A faster decay of the barrier signal and a faster rise of the QW signal are clearly observed in the 70-Å sample.

The inset of Fig. 4 illustrates the simplified scheme of the different relaxation channels of carriers photoexcited

at 2.05 eV. Electron and hole capture times are deduced from a simultaneous fit of the QWL and BL temporal behavior, using the same fitting parameters. Our model considers the evolution equations for the populations of the different levels under the following assumptions: (i) deltalike excitation pulses, (ii) hole cooling to lattice temperature is assumed to be almost instantaneous (≈ 500 fs), (iii) electron relaxation and cooling time is limited by the $L-\Gamma$ scattering time¹⁶ (≈ 2 ps), (iv) recombination in the barriers is neglected. Under these assumptions, we are left with four adjustable parameters: the two capture times, the lifetime (τ_w) of the population in the well, and the proportion (α_{well}) of carriers photoexcited directly in the wells (with large wave vectors). τ_w might vary with the evolution of the carrier populations but this value is roughly given by the long-time behavior deduced from the QW luminescence decay time (typically > 500 ps). The parameter α_{well} which depends on the number of confined and continuum states below the excitation levels is not known precisely. However, estimation from the density of states gives a value of 0.2 for thin wells and 0.5 for larger wells. We therefore obtained the two capture

times, reported in Table I, with fitting curves (solid lines) reported in Fig. 3 for three samples. Altogether the uncertainty, given in Table I, is of the order of $\pm 20\%$ whereas the electron capture times vary by almost 2 orders of magnitude.

We have carried out calculations of the electron capture times using the envelope-function formalism.³ We have considered electron capture mechanisms via LO-phonon emission and via impurity scattering. The scattering rate is computed using the Fermi golden rule. For a given initial wave function, the scattering rate is obtained by summing the interaction integral over all bound states. For LO-phonon scattering, we have considered only phonon emission and we neglect the effect of confined phonon modes. For impurity scattering, a uniform concentration level of 10^{16} impurities per cm^3 , determined by independent measurement, is assumed. The temperature of the carriers (100 K) is taken into account by a proper average over the initial states. No extra fitting parameter has been used in the calculations. Details are given elsewhere.¹³ The results of this calculation are plotted in Fig. 4. For a given Al composition in the barriers, two kinds of resonance are observed. The first resonance (around 63 Å for $x_{\text{Al}}=0.27$) originates from increased barrier and well wave-function overlap when $E_{\text{barr}} \approx E_{\text{well}}(n=2)$. The second resonance (around 71 Å for $x_{\text{Al}}=0.27$) corresponds to the situation where the wave vector of the emitted phonon is approaching zero [$E_{\text{barr}} \approx E_{\text{well}}(n=2) + 36$ meV]. The position of the resonances is very sensitive to the structural parameters; a difference in the alloy composition from 0.27 to 0.31 changes the position of the resonances by almost 10 Å.

It is more difficult to estimate the hole capture times. Quantum-mechanical calculations give capture times longer than for electrons and numerous very narrow reso-

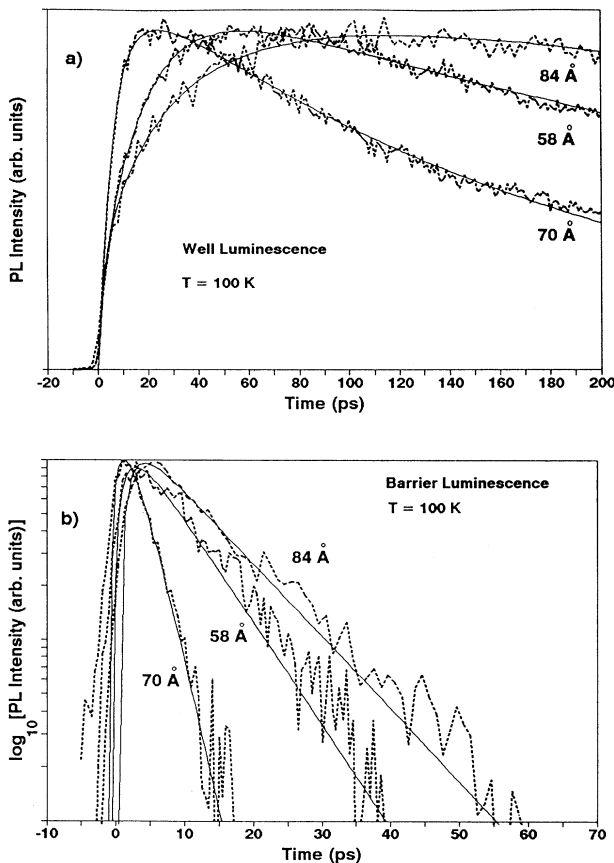


FIG. 3. Time delay behavior at the energy of the $n=1$ well peak (a) and at the energy of the barrier peak (b) for three samples having a well width of 58, 70, and 84 Å (dashed lines). The solid lines correspond to experimental curves obtained using the fitting procedure described in the text.

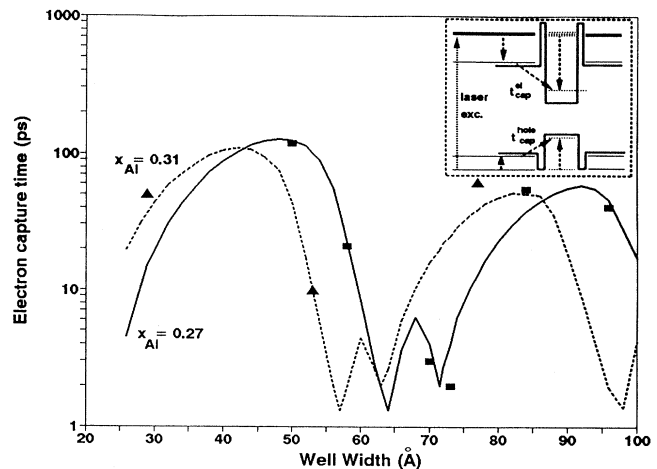


FIG. 4. Theoretical curves of the electron capture time as a function of well width for the barrier configuration shown in Fig. 1 for $x_{\text{Al}}=0.27$ (solid line) and $x_{\text{Al}}=0.31$ (dashed line). Electron capture times deduced from the fitting procedure marked with rectangles (triangles) have to be compared with the theoretical solid (dashed) curve. The inset shows a simplified scheme of the different levels and the different channels of relaxation of the carriers photoexcited at high energy.

nances. However, our calculations suffer from rendering correctly the complex hole band mixing. The band non-parabolicity combined with the well width fluctuations tend to smooth out the resonances and give capture times typically > 100 ps. Such quantum-mechanical calculations are questionable because the length of coherence for the heavy hole is smaller than the period of the structure. In our modified MQW's, the edge spikes tend to localize the heavy holes in the barriers. A semiclassical model gives a better estimation of the hole capture time. We calculate the tunneling time across the edge spike between continuum states without conservation of momentum. Once in the wells, the holes are very easily scattered into lower-energy well states by LO-phonon emission ensuring efficient hole trapping by the wells. The hole capture time estimated in this way is about 3 ps and nearly independent of well width.

In order to interpret the results, we have to consider the capture of both electrons and holes. The observed decay times of the barrier luminescence are weakly dependent on the structure. Fast decay times (< 3 ps) are only observed in the two samples where LO-phonon electron capture resonance is expected (nos. 6 and 7). In all other samples, decay times of typically 10 ps are observed. This result is well explained by the semiclassical model for the hole capture process which gives short hole capture times nearly independent of the structure, and by the quantum-mechanical model for the LO-phonon-assisted electron capture mechanism which gives strong capture time resonances around 70 Å. So in all cases, except for samples nos. 6 and 7, the holes are captured more efficiently than the electrons.

Table I compares the experimental data with the theoretical electron capture times. Also given in Table I is the energy difference between the electron barrier ground state and the last confined level (δE_{el}). These values are determined from an envelope-function calculation of the different levels using the measured sample pa-

rameters and explain the position of the structures observed in luminescence (see Fig. 2). The fitting procedure gives hole capture times smaller than 15 ps and electron capture times oscillating between 2 and 120 ps. The agreement between experimental and theoretical electron capture times is remarkably good. The experimental data are plotted in Fig. 4. Results clearly evidence the $q=0$ LO-phonon resonance (for well width around 71 Å) corresponding to $\delta E_{el} \approx 36$ meV. Unfortunately, the second resonance (around 63 Å for $x_{Al}=0.27$) resulting from the barrier wave-function buildup in the well, has just been missed. Nevertheless, the decreasing capture time obtained for the 53- (31%) and the 58-Å (27%) samples shows that this quantum effect is also present.

In summary, we have used time-resolved luminescence spectroscopy to measure the electron and hole capture time as a function of well width in multiple-quantum-well structures with modified barrier configuration. Results show that holes are captured efficiently in all cases. This is in agreement with our previous results obtained on normal MQW samples.¹³ In the present structure, hole capture process is well described by a semiclassical model. For electrons, we evidence the two kinds of resonance predicted theoretically. The electron capture times are shown to vary between 2 and 120 ps as a function of well width. The quantum-mechanical description for the electron capture mechanism is proved to be valid. Since electron coherence length in our high-quality samples might not be very different from the value expected in normal MQW's, the same conclusion should hold in that case, except that capture times will be smaller by roughly a factor 15.

The authors wish to express their thanks to P. Becker, A. Chomette, F. Clérot, C. Guillemot, and B. Lambert for useful discussions. Thanks also to M. Baudet for her work in the x-ray diffraction pattern fit. One of us (D.M.) thanks Fonds FCAR for financial support.

*On leave from University of Sherbrooke, Dept. of Physics, Sherbrooke, Québec, Canada J1K 2R1.

¹P. W. M. Blom, J. E. M. Haverkort, and J. H. Wolter, *Appl. Phys. Lett.* **58**, 2767 (1991).

²A. Fraenkel, A. Brandel, G. Bahir, E. Finkmann, G. Livescu, and M. T. Asom, *Appl. Phys. Lett.* **61**, 1341 (1992).

³J. A. Brum and G. Bastard, *Phys. Rev. B* **33**, 1420 (1986).

⁴M. Babiker and B. K. Ridley, *Superlatt. Microstruct.* **2**, 287 (1986).

⁵J. A. Brum, T. Weil, J. Nagle, and B. Vinter, *Phys. Rev. B* **34**, 2381 (1986).

⁶S. V. Kozyrev and A. Ya Shik, *Fiz. Tekh. Poluprovodn.* **19**, 1667 (1985) [*Sov Phys. Semicond.* **19**, 1024 (1985)].

⁷N. Ogasawara, A. Fujiwara, N. Ohgushi, S. Fukatsu, Y. Shiraki, Y. Katayama, and R. Ito, *Phys. Rev. B* **42**, 9562 (1990).

⁸J. Feldman, G. Peter, E. O. Göbel, K. Leo, H. J. Polland, K. Ploog, K. Fujiwara, and T. Nakayama, *Appl. Phys. Lett.* **51**, 226 (1987).

⁹B. Deveaud, J. Shah, T. C. Damen, and W. T. Tsang, *Appl.*

Phys. Lett. **52**, 1886 (1988).

¹⁰D. Y. Oberli, J. Shah, J. L. Jewel, T. C. Damen, and N. D. Chand, *Appl. Phys. Lett.* **54**, 1028 (1989).

¹¹S. Weiss, J. M. Wiesenfeld, D. S. Chemla, G. Sucha, M. Wegener, G. Eisenstein, C. A. Burrus, A. G. Dentai, U. Koren, B. I. Miller, H. Temkin, R. A. Logan, and T. Tanbun-Ek, *Appl. Phys. Lett.* **60**, 9 (1992).

¹²R. Kersting, R. Schwedler, K. Wolter, K. Leo, and H. Kurz, *Phys. Rev. B* **46**, 1639 (1992).

¹³B. Deveaud, D. Morris, A. Chomette, and A. Regreny, *Solid State Commun.* (to be published).

¹⁴A. Fujiwara, S. Fukatsu, Y. Shiraki, and R. Ito, *Surf. Sci.* **263**, 642 (1992).

¹⁵A thermalized distribution of carriers is observed within the first 100 fs at excitation densities as low as 10^{17} cm⁻³, see T. Elsaesser, J. Shah, L. Rota, and P. Lugli, *Phys. Rev. Lett.* **66**, 1757 (1991).

¹⁶J. Shah, B. Deveaud, T. C. Damen, W. T. Tsang, A. C. Gosard, and P. Lugli, *Phys. Rev. Lett.* **59**, 2222 (1987).